Available online at www.sciencedirect.com
SCIENCE DIRECT®
C. R. Geoscience 335 (2003) 185–192
COMPTES RENDUS GEOSCIENCE

Geomaterials / Géomatériaux

Evaluation of metallogenic potential of the Nuggihalli greenstone belt, South India

Évaluation du potentiel métallogénique de la ceinture de roches vertes de Nuggihalli, Sud de l'Inde

Sachinath Mitra, Maibam Bidyananda *

Department of Geological Sciences, Jadavpur University, Kolkata 700032, India

Received 16 July 2002; accepted 6 January 2003

Presented by Zdenek Johan

Abstract

Chromite from the north–south-trending schist belt of Nuggihalli (southern Karnataka), belonging to the greenstone belt of South India (3.0–3.5 Ga) and crystallising at 1178 °C under oxygen fugacity of −6.67 shows komatiitic affinity. The chemical data of the Cr-spinels when plotted in the form of the discriminant function of Johan (1979) show a remarkable follow-up of the curve A, which delineates the boundary between the 'barren' and 'fertile' (with respect to the plausible presence of sulphide phases) Cr-spinel bodies. Only a few samples plot marginally within the barren region (Fig. 1), suggesting that the chromite bands should hardly hold the possibility of becoming host of sulphide mineralisation of commercial relevance.

Résumé

La chromite en provenance de la ceinture schisteuse nord–sud de Nuggihalli (Sud de Karnataka), appartenant à la ceinture de roches vertes du Sud de l'Inde (3,0–3,5 Ga), minéral qui cristallise à 1178 °C pour une fugacité de l'oxygène de −6,67, montre une affinité komatiitique. Lorsque les données chimiques relatives aux spinelles chromifères sont représentées sous la forme d'une fonction discriminante de Johan (1979), elles suivent remarquablement la courbe A, qui délimite les corps « stériles » et « fertiles » de spinelles ferrifères (en fonction de la présence possible de phases sulfurées). Seuls les points représentatifs de quelques échantillons tombent marginalement dans la région stérile (Fig. 1), suggérant que les bandes de chromite pourraient difficilement devenir des minéraux hôtes d'une minéralisation sulfurée d'intérêt commercial.

Keywords: Chromite; Metallogenic potential; Greenstone belt; South India

Mots-clés : Chromite ; Potentiel métallogénique ; Ceinture de roches vertes ; Sud de l'Inde

* Corresponding author. Present address: Planetary and Geosciences Division, Physical Research Laboratory, Ahmedabad-380009, India.
E-mail address: maibam@prl.ernet.in (M. Bidyananda).

1631-0713/03/$ – see front matter
doi:10.1016/S1631-0713(03)00034-8

1. Introduction

Johan [11] investigated the compositional plane of spinels (Fe_3O_4–$FeCr_2O_4$–$MgAl_2O_4$) and found that spinels showing an association with sulphides such as Cu–Ni sulphides, are characterised by Mg–Al cationic relations as $2\,\mathrm{Mg}-\mathrm{Al} < 0$, whereas those which are barren (no mineralisation of sulphides or such) should show $2\,\mathrm{Mg}-\mathrm{Al} > 0$. In the model, Johan developed a discriminant function:

$$G = \mathrm{Cr}\,(\mathrm{Al} + \mathrm{Fe}^{2+})/(\mathrm{Fe}^{2+}\,\mathrm{Al}) = (0.711/X - 1.11\,X)/(1 - X)$$

with $X = \mathrm{Mg}/(\mathrm{Mg} + \mathrm{Fe}^{2+})$.

The function is graphically represented as curve A in Fig. 1. Spinels, devoid of sulphide (or such) phases, should plot above this curve while those with such mineralisation should plot below this curve.

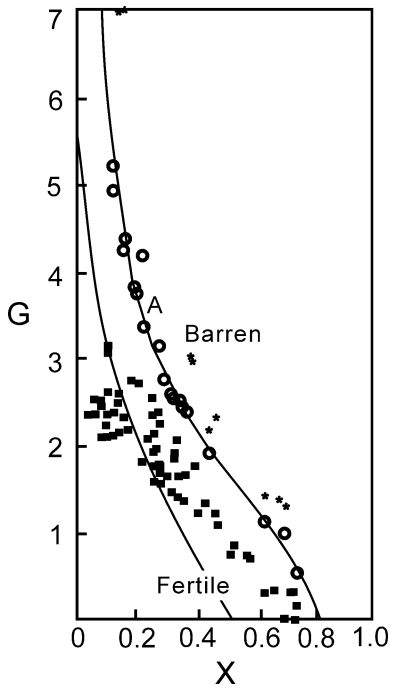

Fig. 1. Graphical expression (curve A) of the $G:\mathrm{Cr}(\mathrm{Al} + \mathrm{Fe}^{2+})/(\mathrm{Fe}^{2+}\,\mathrm{Al}) = (0.711/X - 1.111\,X)/(1 - X)$ with $X = \mathrm{Mg}/(\mathrm{Mg} + \mathrm{Fe}^{2+})$. Staré Ransko spinels (■), Horni Bory spinels (⋆) and Nuggihalli spinels (○).

Fig. 1. Expression graphique (courbe A) de $G:\mathrm{Cr}(\mathrm{Al} + \mathrm{Fe}^{2+})/(\mathrm{Fe}^{2+}\mathrm{Al}) = (0{,}711/X - 1{,}111\,X)/(1 - X)$ avec $X = \mathrm{Mg}/(\mathrm{Mg} + \mathrm{Fe}^{2+})$. Spinelles de Staré Ransko (■), spinelles de Horni Bory (⋆) et spinelles de Nuggihalli (○).

With strange serendipity, the chemistry of different grains of a series of samples collected from the chromite bodies of Nuggihalli (stretching nearly north–south over a distance of 50 km) was observed to plot remarkably on the demarcating line and thereby prove the ingenuity of Johan in postulating the trend.

2. Geology of the study area

The Nuggihalli schist belt (3.0–3.5 Ga; e.g., [14]) occurs as a band of low-grade metamorphosed ultramafic bodies stretching roughly NW–SE to north–south in the Dharwar craton, belongs to the greenstone belt in South India (see map, Fig. 2). Ultramafic rocks of the area consist of unaltered dunite, harzburgite, chromite bearing serpentinite, and talc–chlorite–tremolite schist. Other major rock types are amphibolite, metasediments (fuchsite quartzite, quartz–mica–chlorite schist and staurolite–quartz–mica schist), tonalite trondhjamitic gneisses and meta-anorthosite. Titanomagnetite bodies rich in vanadium are intercalated with the ultramafic rocks. The area under study has been subjected to greenschist-to-amphibolite facies metamorphism and shows increase in grade from north to south [19].

The chromite bodies occur commonly as layers, high angle bands and in irregular tabular or lensoid forms within serpentinite. The size of the chromite deposit varies from lenticular bands ∼300 m in length, with a width of 6 m at Tagadur mines and pods of a few metres to more than 60 m size, extending to a depth of ∼100 m in Byrapur underground mine. The spectacular rosy moss-like aggregates of pink chlorite (Cr-bearing clinochlore) occur as veins and fracture fillings and as pockets in grey chromite ore bodies [4]. Based on the presence of pillow structure and spinifex texture in peridotite, Naqvi and Hussain [15] suggested submarine extrusion to have occurred. From the Cr/Al ratio in serpentinite, komatiitic affiliation was deciphered by Sudhakar [22]. The identification of a komatiitic affinity for the ultramafic rocks of the belt led to the suggestion by these investigators that this belt is an example of Barberton type greenstone belt, in which the komatiitic rocks are considered to

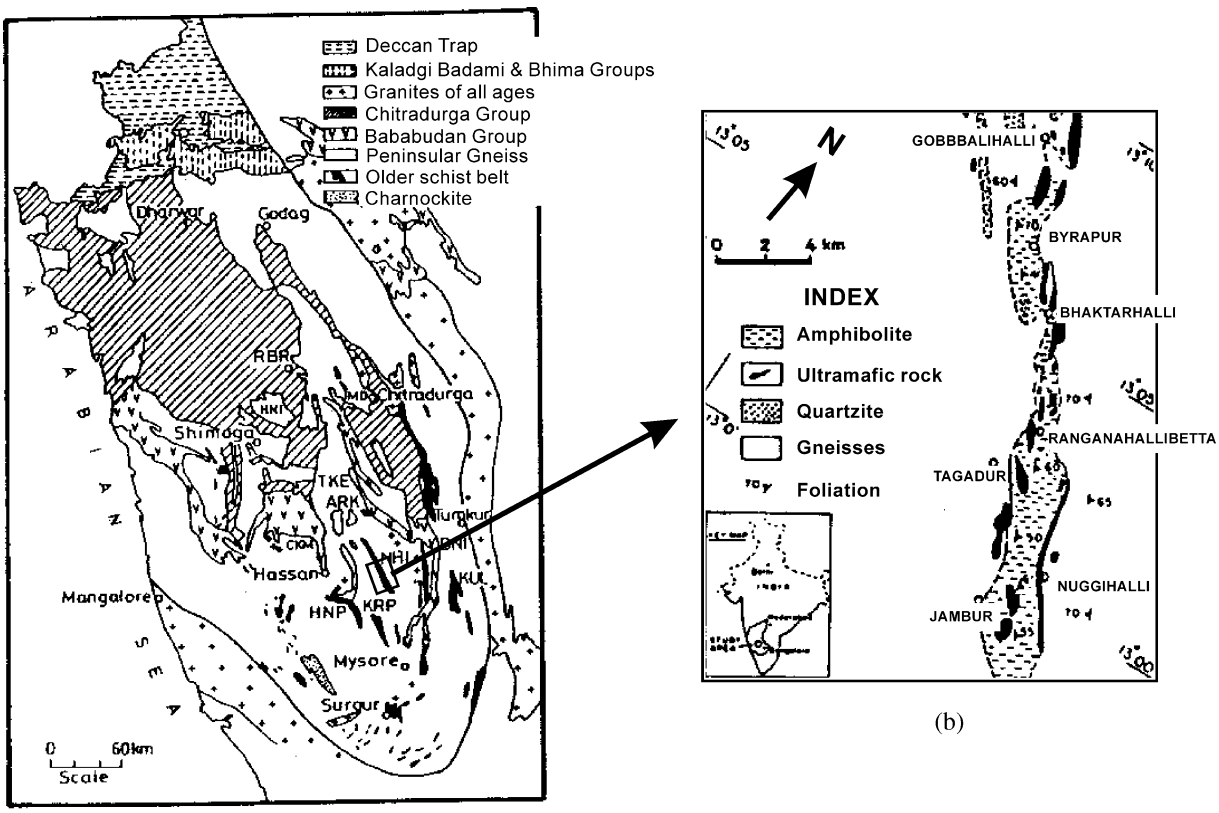

Fig. 2. (**a**) Geological map of part of the Dharwar craton following Radhakrishna and Naqvi [18]. **NHI:** Nuggihalli; **KUL:** Kunigal; **KRP:** Krishnarajpet; **HNP:** Holenarasipur; **RBR:** Ranibennur. (**b**) Geological map showing section of the Nuggihalli schist belt from which the samples have been collected (modified from [10]).

Fig. 2. (**a**) Carte géologique d'une partie du craton de Dharwar selon Radhakrishna et Naqvi [18]. **NHI :** Nuggihalli ; **KUL :** Kunigal ; **KRP :** Krishnarajpet ; **HNP :** Holenarasipur ; **RBR :** Ranibennur. (**b**) Carte géologique montrant une coupe de la ceinture schisteuse de Nuggihalli, dont sont issus les échantillons étudiés (modifié d'après [10]).

be pristine and primordial. The Cr/Fe ratio of chromite indicates a layered intrusion complex [16].

Probable stratigraphic succession of the belt modified from the one reported by Jafri et al. [10] is presented below:

- dolerite dyke,
- meta-anorthosite,
- gneisses,
- dunite,
- titanomagnetite, gabbro, metasediments,
- amphibolite,
- perodotite/serpentinite, with bands of chromite, tremolite–talc schist.

3. Chemical study

The chromite samples were collected from chromitite bodies which run as bands and lenses within serpentinised masses. The chromite samples were chemically analysed by a JEOL-733 electron microprobe with wavelength dispersive method at 15 kV with a beam current of 10 nA and a beam diameter of 10 μm. Average spectrum counts (10 s × 5 times) were compared with natural standards and data were corrected by the Bence and Albee method [3]. The minerals that were used as the standards are; albite for Si and Na, almandine for Al and Fe, olivine for Mg, rhodonite for Mn, rutile for Ti, diopside for Ca and sanidine for K.

Table 1
Average chemical formulae of the Cr-spinels from Nuggihalli schist belt

Tableau 1
Formules chimiques moyennes des spinelles chromifères de la ceinture schisteuse de Nuggihalli

Gob 7i	$(Fe^{2+}_{5.054}\,Fe^{3+}_{0.576}\,Mg_{2.836}\,Cr_{10.919}\,Al_{4.562}\,Ti_{0.045}\,Mn_{0.158}\,Ni_{0.007}\,Na_{0.002}\,Ca_{0.005}\,Si_{0.026})O_{32}$
Gob 7ii	$(Fe^{2+}_{5.150}\,Fe^{3+}_{0.498}\,Mg_{2.706}\,Cr_{11.737}\,Al_{3.847}\,Ti_{0.026}\,Mn_{0.183}\,Ni_{0.009}\,Na_{0.006}\,Si_{0.011})O_{32}$
G1	$(Fe^{2+}_{6.197}\,Fe^{3+}_{1.000}\,Mg_{1.768}\,Cr_{8.344}\,Al_{6.796}\,Ti_{0.026}\,Mn_{0.133})O_{32}$
†***By 3***	$(Mg_{3.550}\,Si_{0.006}\,Mn_{0.094}\,Fe^{2+}_{1.667}\,Fe^{3+}_{2.298}\,Ni_{0.009})(Al_{2.007}\,Ti_{0.095}\,Cr_{12.020}\,Fe^{2+}_{1.164})O_{32}$
By 5	$(Fe^{2+}_{6.119}\,Fe^{3+}_{0.979}\,Mg_{1.773}\,Cr_{12.255}\,Al_{2.955}\,Ti_{0.037}\,Mn_{0.180}\,Ni_{0.022}\,Ca_{0.016}\,K_{0.012}\,Si_{0.009})O_{32}$
By	$(Fe^{2+}_{6.417}\,Fe^{3+}_{1.596}\,Mg_{1.606}\,Cr_{12.240}\,Al_{2.416}\,Ti_{0.128}\,Mn_{0.103})O_{32}$
By 1	$(Fe^{2+}_{6.401}\,Fe^{3+}_{1.642}\,Mg_{1.483}\,Cr_{12.348}\,Al_{1.999}\,Mn_{0.119}\,Ni_{0.008})O_{32}$
B	$(Fe^{2+}_{2.677}\,Fe^{3+}_{0.499}\,Mg_{5.283}\,Cr_{11.657}\,Al_{3.880}\,Ti_{0.042}\,Mn_{0.065})O_{32}$
†***T4***	$(Mg_{3.089}\,Si_{0.046}\,Mn_{0.155}\,Fe^{2+}_{1.789}\,Fe^{3+}_{2.916}\,Ni_{0.005})(Mg_{0.909}\,Al_{2.679}\,Ti_{0.054}\,Cr_{10.189}\,Fe^{2+}_{1.527})O_{32}$
Tag 4i	$(Fe^{2+}_{3.928}\,Fe^{3+}_{2.284}\,Mg_{3.521}\,Cr_{12.331}\,Al_{2.231}\,Ti_{0.124}\,Mn_{0.104}\,Ni_{0.020}\,Na_{0.004}\,Si_{0.024})O_{32}$
Tag 4ii	$(Fe^{2+}_{5.782}\,Fe^{3+}_{1.123}\,Mg_{1.996}\,Cr_{12.296}\,Al_{2.879}\,Ti_{0.026}\,Mn_{0.187}\,Ni_{0.011}\,K_{0.008}\,Si_{0.041})O_{32}$
T	$(Fe^{2+}_{5.061}\,Fe^{3+}_{0.394}\,Mg_{2.821}\,Cr_{10.655}\,Al_{4.973}\,Ti_{0.048}\,Mn_{0.151})O_{32}$
T6	$(Fe^{2+}_{5.096}\,Fe^{3+}_{0.481}\,Mg_{2.735}\,Cr_{10.800}\,Al_{4.668}\,Mn_{0.160}\,Ni_{0.010})O_{32}$
J2	$(Fe^{2+}_{5.772}\,Fe^{3+}_{0.669}\,Mg_{2.145}\,Cr_{10.925}\,Al_{4.548}\,Ti_{0.018}\,Mn_{0.153})O_{32}$
†***J1***	$(Mg_{1.391}\,Si_{0.023}\,Mn_{1.391}\,Fe^{2+}_{1.554}\,Fe^{3+}_{3.108}\,Ni_{0.015})(Mg_{5.278}\,Ti_{0.023}\,Cr_{8.862}\,Fe^{2+}_{1.774})O_{32}$
J4	$(Fe^{2+}_{5.332}\,Fe^{3+}_{1.671}\,Mg_{2.688}\,Cr_{10.388}\,Al_{4.056}\,Ti_{0.289}\,Ni_{0.036}\,Na_{0.002}\,Ca_{0.056}\,Si_{0.794})O_{32}$
Jam 6i	$(Fe^{2+}_{6.020}\,Fe^{3+}_{2.205}\,Mg_{1.571}\,Cr_{12.253}\,Al_{2.291}\,Ti_{0.120}\,Mn_{0.114}\,Ni_{0.011}\,K_{0.004}\,Na_{0.005}\,Si_{0.008})O_{32}$
Jam 6ii	$(Fe^{2+}_{6.126}\,Fe^{3+}_{3.161}\,Mg_{1.328}\,Cr_{12.723}\,Al_{1.228}\,Ti_{0.142}\,Mn_{0.126}\,Ni_{0.013}\,K_{0.007}\,Na_{0.020}\,Si_{0.012})O_{32}$
JCM 3	$(Fe^{2+}_{6.990}\,Fe^{3+}_{2.698}\,Mg_{1.024}\,Cr_{13.136}\,Al_{0.632}\,Ti_{0.081}\,Mn_{0.208}\,Ni_{0.096})O_{32}$

Iron as Fe^{3+} and Fe^{2+} calculated from ideal spinel stoichiometry. †Fe^{2+} and Fe^{3+} determined from Mössbauer spectroscopy.

Table 1 shows the chemistry of studied chromites. Detail chemistry of relict and metamorphosed mineral phases (viz., olivine, pyroxene, amphibole, chlorite, etc.) will be presented in a subsequent paper.

We have plotted the chromite chemistries in $100 \times Cr/(Cr + Al)$ (Cr^*) vs $100 \times Mg/(Mg + Fe^{2+})$ (Mg^*), which revealed that the studied samples fall in the cluster of the well-known stratiform deposits of the world. The modified $100 \times Fe^{3+}/(Cr + Al + Fe^{3+})$ ($Fe^{3+\bullet}$) vs $100 \times Mg/(Mg + Fe^{2+})$ (Fig. 3) and Cr_2O_3 vs Al_2O_3 wt% (Fig. 4a) plots show the komatiitic affinity of the chromitite bodies. However, FeO (total) vs Cr_2O_3 (Fig. 4b) simultaneously brings out its continental layered characteristics. From these plots, it can be emphasised that the chromite from the komatiites and stratiform deposits fall in the same compositional field. We have used Rollinson's $Cr/(Cr + Al)$ vs $Fe^{2+}/(Fe^{2+} + Mg)$ plot [20] (Fig. 5) to compare the studied chromitites with reported komatiitic chromitite of Zimbabwe (Belingwe, Inyala and Shurugwi). They all fall in the same range ($Cr/(Cr + Al)$ varying from 0.6 to 0.9 whereas $Fe^{2+}/(Fe^{2+} + Al)$ from 0.26 to 0.87) as reported. This comparison is instructive, because the mentioned komatiites are the most studied and offer the best opportunity to study primary magmatic mineral deposits. We have also plotted our chromite data in the Barnes and Roeder [2] longitudinal spinel projections of $Cr/(Cr + Al)$ and $Fe^{3+}/(Cr + Al + Fe^{3+})$ vs $Fe^{2+}/(Mg + Fe^{2+})$ and TiO_2 vs $Fe^{3+}/(Cr + Al + Fe^{3+})$ diagrams. All the studied samples show their komatiitic affinity.

4. Thermal history of the chromite

The chromite–olivine assemblage has been used to determine the temperature of formation of the chromite ores. The calibration proposed by Fabries [8] has been used to determine the temperature in the present study. This thermometer is successfully

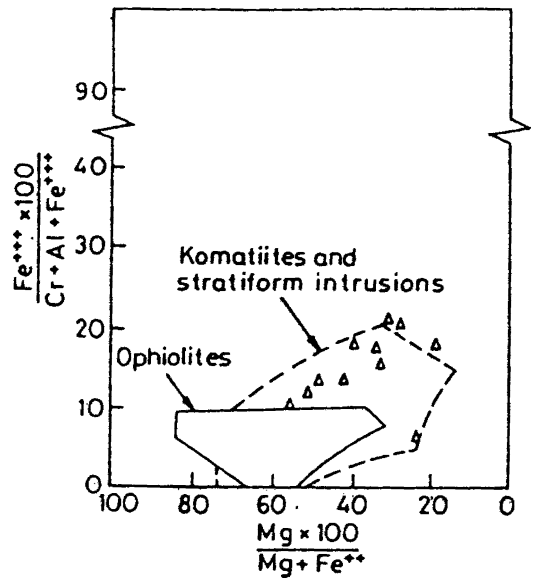

Fig. 3. Composition of chromite plotted on projections of the spinel prism of Steven's [21]. The fields for the various types of complexes shown are based on [5,7,9,24].

Fig. 3. Compositions de chromite représentées sur des projections de prisme des spinelles de Steven [21]. Les champs des différents types de complexes représentés sont basés sur les données de [5,7, 9,24].

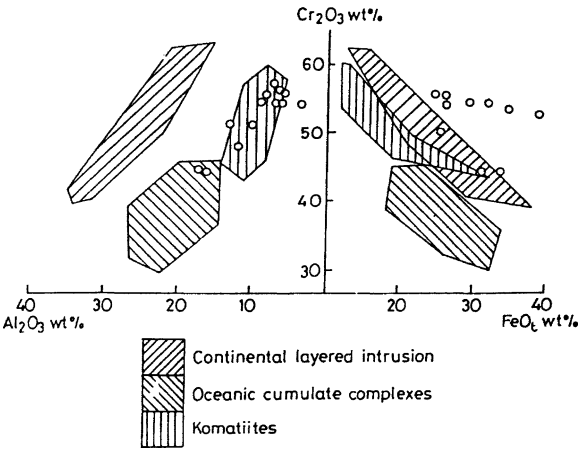

Fig. 4. Discrimination diagrams for chromite composition plotted in terms of Cr_2O_3 vs Al_2O_3 and Cr_2O_3 vs FeO_t. Modified from a four-component diagram of [1].

Fig. 4. Diagrammes de discrimination pour des compositions de chromite représentées en termes de Cr_2O_3 vs Al_2O_3 et Cr_2O_3 vs FeO_t. Modifié à partir d'une diagramme à quatre composants [1].

applied to the olivine having Fo content ∼90% and it has reasonably been used in the present case, since the Fo content of the olivine (83–92%) is close to that value. Detail chemistry will be presenting elsewhere. The thermometric relation is:

$$T = \frac{4250\,\gamma_{Cr}^{sp} + 1343}{\ln K_D^0 + 1.825\,\gamma_{Cr}^{sp} + 0.571}$$

where K_D^0 is the apparent distribution coefficient, with $\ln K_D^0 = \ln K_D - 4.0\,\gamma_{Fe}^{sp}$.

In the above equation,

$$K_D = \frac{X_{Mg}^{ol}\,X_{Fe}^{sp}}{X_{Fe}^{ol}\,X_{Mg}^{sp}}$$

$$\gamma_{Cr}^{sp} = \left(Cr/\sum \text{ octahedral cations}\right)^{sp}$$

In the present case, the chemistry of coexisting olivine and chromite from a sample (JCM 3, the composition of which would be presented elsewhere), is used for the calibration and the following values are obtained:

$$X_{Mg}^{sp} = 0.474, \quad X_{Fe}^{sp} = 0.517, \quad X_{Mg}^{ol} = 0.890,$$
$$X_{Fe}^{ol} = 0.109, \quad \gamma_{Cr}^{sp} = 0.759, \quad \gamma_{Fe^{3+}}^{sp} = 0.222,$$
$$K_D = 8.868, \quad \ln K_D = 2.18, \quad \ln K_D^0 = 1.292$$

The Fe^{2+} and Fe^{3+} contents in chromites have been based on stoichiometric calculations. Using the above equation, the temperature of formation of Nuggihalli chromite has been determined as 1178 °C.

5. The f_{O_2} determination

The oxygen fugacity of the chromite from the Nuggihalli schist belt has been determined by the method discussed in [13]. According to this method the f_{O_2} is determined from $Fe^{3+}/(Cr + Al + Fe^{3+})$ ratio of chromite owing to its strong dependence on f_{O_2} and very weak dependence on the melt composition. To determine the f_{O_2} of Stillwater and Bushveld complex, some [13] used this method, the results of which are consistent to the estimation by other methods. The f_{O_2}–T paths of natural basalt are sub-parallel to QFM (quartz–fayalite–magnetite) buffer curves [6]; therefore, f_{O_2} of natural magma decreases with decreasing temperature. For this reason, to eliminate the normal temperature effect f_{O_2} values are expressed relative

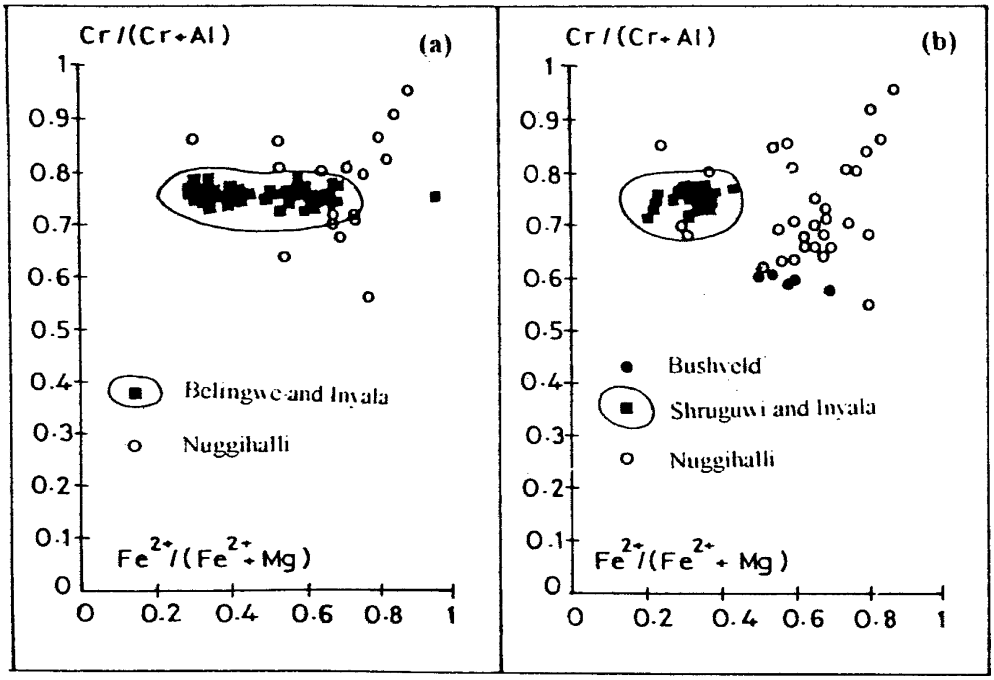

Fig. 5. Cr/(Cr + Al) vs $Fe^{2+}/(Fe^{2+} + Mg)$ [20] plots of the studied Cr-spinels in comparison with chromitites from komatiites of (**a**) Inyala and Belingwe greenstone belts, Zimbabwe (**b**) Inyala, Shruguwi, Zimbabwe and Bushveld intrusion, South Africa.

Fig. 5. Diagrammes de Cr/(Cr + Al) en fonction de $Fe^{2+}/(Fe^{2+} + Mg)$ [20] par les spinelles chromifères étudiés, comparés aux chromitites des kromatiites (**a**) des ceintures de roches vertes d'Inyala et de Belingwe, Zimbabwe, (**b**) de l'intrusion d'Inyala, Shruguwi du Zimbabwe et du Bushveld, en Afrique du Sud.

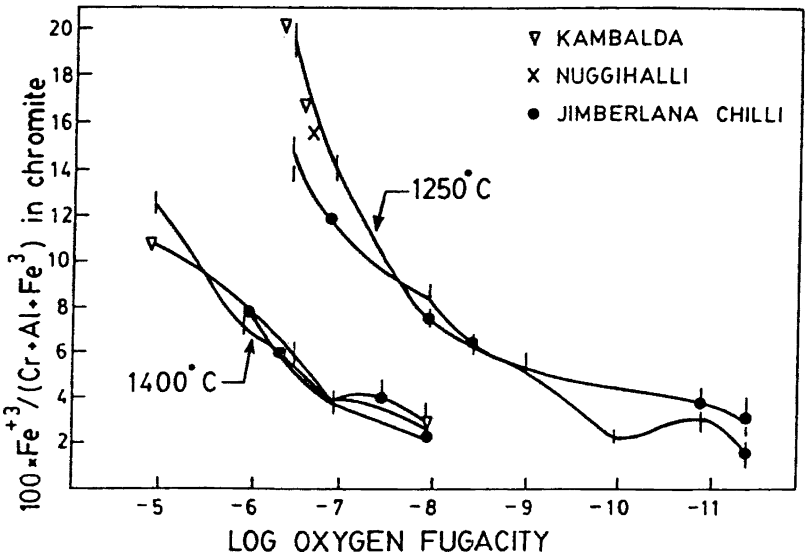

Fig. 6. $100 \times Fe^{3+}(B)/[Cr + Al(B) + Fe^{3+}(B)]$ (atomic proportion) in chromites as a function at 1250 °C and 1400 °C (after [13]).

Fig. 6. $100 \times Fe^{3+}(B)/[Cr + Al(B) + Fe^{3+}(B)]$ en fonction de la fugacité de l'oxygène à 1250 °C et 1400 °C (selon [13]).

to one of buffer curves. Error in 200 °C temperature of crystallisation makes an error in f_{O_2} values only of 0.5 log unit. The EPMA and Mössbauer study lead to the determination of $100 \times Fe^{+3}/(Al + Cr + Fe^{3+})$ as 15.6. The temperature of formation of Nuggihalli chromite has been determined from olivine–spinel geothermometer as 1178 °C. Since most of the chromitite layers form within 1250 ± 100 °C, curves at that temperature of Fig. 6 are reasonable [13]. Therefore, the 1250 °C curve of Fig. 6 has been used to determine log f_{O_2}, which comes as -6.67.

6. Discussion

The Nuggihalli chromite which crystallises at $\sim$ 1180 °C with an oxygen fugacity of -6.67, appearing from their chemical plots (Figs. 3–5) indicates their komatiitic affinity. Working on the Cr-spinels from the Staré Ransko gabbro-peridotite, Czech Republic, van der Veen and Maaskant [23] reported that all the spinels from the investigated samples plotted below the discriminant curve A (Fig. 1), which indicates a strong possibility for sulphide mineral association. This indeed was true. While the spinels from the Horni Bory xenoliths [12], showing no evident presence of sulphides etc. plotted distinctly above the discriminant curve. Much to the surprise of the present authors the spinels of Nuggihalli plot remarkably along the curve itself. This observation reinforces the logic of van der Veen and Maaskant [23] and redefines the validity of the profile of the boundary curve of Johan [11].

Fig. 1 shows that all the spinels from Nuggihalli schist belt plot on the discriminant curve A but a few plot within the barren zone close to the A curve. This evidently points the possibility of chromitite band (along with its silicate host rocks) being barren rather than fertile. This observation eliminates the strong possibility for chromitite to host any mineralisation of sulphides or their kind.

The reported occurrence of sulphides [17] (chalcopyrite, pyrite, pyrrhotite, cubanite and pentlandite) in the close proximity of the ultramafic intrusions in this belt is inevitably seen to be confined within the marginal part of gabbroic masses, intrusive into the ultramafic (later metamorphosed) bodies hosting the chromite and titanomagnetite bands.

The validity of the discriminant curve A of Johan [11] thus receives a further endorsement from the chromite characters of the greenstone belt of south India.

Acknowledgements

The authors express sincere thanks to Prof. H.S. Moon of Yonsei University, Seoul, for the EPMA analyses, and Mysore Minerals Ltd. for all cooperation in the field work. Authors are much thankful to the two anonymous reviewers for constructive and encouraging reviews. Thanks to Department of Science and Technology, Govt. of India for the financial support.

References

[1] W.E. Bai, M.F. Zhou, Variations in chemical compositions of chrome spinels from Hongguleleng ophiolites, Xianjing, China and their significance, Acta Mineral. Sin. 8 (1988) 313–323 (in Chinese).
[2] S.J. Barnes, P.L. Roeder, The range of spinel compositions in terrestrial mafic and ultramafic rocks, J. Petrol. 42 (12) (2001) 2279–2302.
[3] A.E. Bence, A.L. Albee, Empirical correction factors for the electron microanalysis of silicates and oxide, J. Geol. 76 (1968) 382–403.
[4] M. Bidyananda, Petrological and crystallochemical studies of the chromite and magnetite bearing litho-units in the Nuggihalli schist belt (Karnataka): their thermodynamic parameters and geotectonic evolution, PhD thesis, Jadavpur University, 2000, 308 p. (unpublished).
[5] J.C. Bird, A.L. Clark, Microprobe study of olivine chromitites of the Goodnews Bay ultramafic complex, Alaska, and the occurrence of the platinum, US Geol. Surv. J. Res. 4 (1976) 717–725.
[6] I.S.E. Carmichael, F.J. Turner, J. Verhoogen, Igneous Petrology, McGraw-Hill, 1974.
[7] H.J.B. Dick, T. Bullen, Chromian spinel as petrogenetic indicator in abyssal and alpine-type peridotites and spatially associated lavas, Contrib. Mineral. Petrol. 86 (1984) 54–76.
[8] J. Fabriès, Spinel–olivine geothermometry in peridotites from ultramafic complex, Contrib. Mineral. Petrol. 69 (1979) 329–336.
[9] T.N. Irvine, Chromium spinel as a petrogenetic indicator. Part I: Theory, Can. J. Earth Sci. 2 (1967) 648–672.
[10] S.H. Jafri, N. Khan, S.M. Ahmed, R. Saxena, Geology and geochemistry of Nuggihalli schist belt, Dharwar craton, Karnataka, India, in: S.M. Naqvi, J.J.W. Rogers (Eds.), Precambrian of South India, Geol. Soc. Ind. Mem. 4 (1983) 110–120.
[11] Z. Johan, Possibilité de discrimination des massifs basiques minéralisés en nickel et cuivre et des massifs stériles par l'é-

tude cristallochimique des spinelles, in: M. Besson (Ed.), Facteurs contrôlant les minéralisations sulfurées de nickel, Mém. BRGM 97, Chapter 3, Part II, 1979, pp. 203–218.
[12] Z. Misar, E. Jelinek, P. Jakeš, Inclusions of peridotite, pyroxenite and eclogite in granulite rocks of pre-Hercynian upper mantle and lower crust in the eastern Bohemian Massif (Czechoslovakia), Ann. Sci. Univ. Clermont-Ferrand-2 74 (1984) 85–95.
[13] B.W. Murck, I.H. Campbell, The effects of temperature, oxygen fugacity and melt composition on the behaviour of chromium in basic and ultrabasic melts, Geochim. Cosmochim. Acta 50 (1986) 1871–1888.
[14] S.M. Naqvi, J.J.W. Rogers, Precambrian Geology of India, Oxford University Press, Oxford, UK, 1987, 223 p.
[15] S.M. Naqvi, S.M. Hussain, Geochemistry of meta-anorthosites from a greenstone belt in Karnataka, India, Can. J. Earth Sci. 16 (1979) 1254–1264.
[16] R. Nijagunappa, C. Naganna, Nuggihalli schist belt in the Karnataka craton: an Archaean layered complex as interpreted from chromite distribution, Econ. Geol. 79 (1983) 507–513.
[17] B.P. Radhakrishna, S. Achuta Pandit, K.T. Prabhakar, Copper mineralisation in the ultrabasic complex of Nuggihalli, Hassan District, Mysore State, J. Geol. Soc. Ind. 14 (1973) 302–312.
[18] B.P. Radhakrishna, S.M. Naqvi, Precambrian continental crust of India and its evolution, J. Geol. 94 (1986) 145–166.
[19] M. Ramakrishnan, Nuggihalli and Krishnarajpet belts, in: J. Swami Nath, M. Ramakrishnan (Eds.), Early Precambrian Supracrustals of Southern Karnataka, Geol. Surv. Ind. Mem. 112 (1981) 61–70.
[20] H. Rollinson, The Archean komatiite-related Inyala chromitite, Southern Zimbabwe, Econ. Geol. 92 (1997) 98–107.
[21] R.T. Stevens, Composition of some chromites of the Western Hemisphere, Am. Mineral. 29 (1944) 1–34.
[22] K.S. Sudhakar, Pillow structures in serpentinites, Tagadur, Nuggihalli schist belt, Karnataka, Indian Acad. Sci. Proc. Earth Planet. Sci. 89 (1980) 117–119.
[23] A.H. van der Veen, P. Maaskant, Chromian spinel mineralogy of the Staré Ransko gabbro-peridotite, Czech Republic, and its implications for sulfide mineralization, Mineral. Deposita 30 (1995) 397–407.
[24] M.F. Zhou, R. Kerrich, Morphology and composition of chromite in komatiites from the Belingwe greenstone belt, Zimbabwe, Can. Mineral. 30 (1992) 303–317.